Chemical Science

ROYAL SOCIETY OF CHEMISTRY

EDGE ARTICLE

View Article Online
View Journal | View Issue

Cite this: *Chem. Sci.*, 2026, **17**, 8160

All publication charges for this article have been paid for by the Royal Society of Chemistry

Received 9th January 2026
Accepted 21st February 2026

DOI: 10.1039/d6sc00248j

rsc.li/chemical-science

Unexpected dispersion-stabilized tris(terphenylthiolate) complexes, $Ln(SAr^{iPr6})_3$, arising from two-electron reduction by $Ln(SAr^{iPr6})_2$ [Ar^{iPr6} = C_6H_3-2,6-(C_6H_2-2,6,4-$^iPr_3$)$_2$]†

Makayla R. Luevano, ‡ Cary R. Stennett, ‡ Eric Ma, Joseph W. Ziller, Filipp Furche * and William J. Evans *

The first examples of a $M(EAr^{iPr6})_3$ complex [Ar^{iPr6} = C_6H_3-2,6-(C_6H_2-2,4,6-$^iPr_3$)$_2$] of any metal with any donor, E = O, S, NH, PH, have been isolated from the two-electron reduction of 1,3,5,7-cyclooctatetraene by the Ln(II) complexes $Ln(SAr^{iPr6})_2$ [Ln = La, Nd]. Two equiv. of $Ln(SAr^{iPr6})_2$ react with C_8H_8 to form the $(C_8H_8)^{2-}$–ligated Ln(III) complexes, $Ln(SAr^{iPr6})(C_8H_8)$. Surprisingly, the second product of this reaction is the tris(terphenylthiolate), $Ln(SAr^{iPr6})_3$, a complex expected to be too sterically crowded to exist. A computational study showed that interligand London dispersion effects (LDEs) in $Ln(SAr^{iPr6})_3$ are responsible for approximately half of the dissociation energy of the thiolate ligands. Overall, the results demonstrate that the $(SAr^{iPr6})^{1-}$ ligand platform has a wide range of electronic and steric flexibility in rare-earth metal complexes.

Introduction

Historically, the redox chemistry of rare-earth metals, *i.e.* Sc, Y, and the lanthanides, has been criticized for being limited due to the scarce number of oxidation states that are available to these elements.[1–7] For many years, the only oxidation states known in isolable molecular species beyond the most stable +3 oxidation state were Ce(IV), Sm(II), Eu(II), and Yb(II).[8] Since the redox reactions of these ions consisted of one-electron transformations, they were assumed to be unable to accomplish the two-electron redox chemistry that is so productive with transition metals.

However, reactivity studies focusing on Ln(II) metallocenes showed that two electron reduction chemistry could be readily accomplished with rare-earth elements simply by using two equiv. of Ln(II) one-electron reductants.[4] For example, Ln(II) metallocenes, $(C_5R_5)_2Ln(THF)_n$ (n = 0, 2), are known to have an extensive two-electron reductive chemistry as shown in the formation of a homologated dianion of CO in eqn (1).[9,10]

When the two-electron reduction reactivity of $(C_5Me_5)_2$-Sm was investigated with 1,3,5,7-cyclooctatetraene, the reaction generated the first example of a tris(pentamethylcyclopentadienyl) complex of any element, the sterically crowded $(C_5Me_5)_3Sm$, eqn (2).[11] Previously, on the basis of the 142° cone angle of the $(C_5Me_5)^{1-}$ ligand,[12] it was thought that only two of these groups can be attached to a metal even for the largest metal atoms.[13,14]

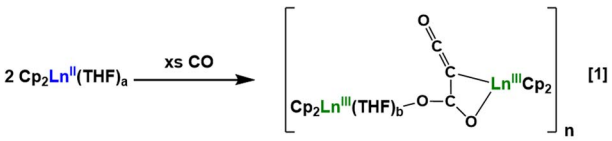

Ln = Sm; Cp = C_5Me_5; a = 2; b = 1; n = 2 (ref 9)
Ln = Tm; Cp = $C_5H_2{}^tBu_3$; a = b = 0; n = 1 (ref 10)

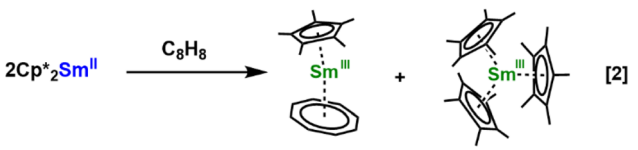

In recent years, the number of oxidation states available in molecular species of rare-earth elements has increased dramatically[15–22] and extensive studies are in progress to identify two-electron redox processes.[20,23–25] We were intrigued to determine if the recently reported[26] neutral La(II) and Nd(II) complexes of the terphenylthiolate ligand, $Ln(SAr^{iPr6})_2$ [Ar^{iPr6} = C_6H_3-2,6-(C_6H_2-2,4,6-$^iPr_3$)$_2$], could participate in two-electron reduction chemistry. If the reaction proceeds as in eqn (2), this would require the formation of $Ln(SAr^{iPr6})_3$ products. However, to our knowledge, no tris(SAr^{iPr6}) complexes, *i.e.* $M(SAr^{iPr6})_3$ of any element, M, have been reported, nor have the phenolate or amide

Department of Chemistry, University of California, Irvine, California 92697-2025, USA. E-mail: wevans@uci.edu

† This work is dedicated to Professor Philip Power, whose pioneering research in exploratory synthesis among the main group and transition elements was inspirational to this effort.

‡ M. R. L and C. R. S. contributed equally to this work.

analogs, $M(OAr^{iPr6})_3$ and $M[N(H)Ar^{iPr6}]_3$, been identified, although examples of Ln(III) complexes coordinating three of the unsubstituted terphenolate ligand, 2,6-diphenylphenoxide, were reported by Deacon and co-workers as early as 1990.[27–30] Alternatively, a $Ln(SAr^{iPr6})_2$ complex could function as a two-electron reductant if a $(SAr^{iPr6})^{1-}$ ligand provided an electron and formed an SAr^{iPr6} radical which could then dimerize to the disulfide $Ar^{iPr6}S—SAr^{iPr6}$. The formation of the disulfide seemed most reasonable since Goodwin, *et al.* recently reported that it formed in a U(IV) reaction[31] and Power, *et al.* had reported that the more highly substituted disulfide $Ar^{iPr8}S—SAr^{iPr8}$ formed during the synthesis of the plumbylene $Pb(SAr^{iPr8})_2$ (Ar^{iPr8} = C_6H-2,6-(C_6H_2-2,4,6-^{i}Pr$_3$)$_2$-3,5-^{i}Pr$_2$).[32] To determine the two-electron reductive capacity of $Ln^{II}(SAr^{iPr6})_2$, we examined its reactivity with 1,3,5,7-cyclooctatetraene.

Results and discussion

Two electron reduction of C_8H_8

Treatment of dark brown diethyl ether solutions of $Ln^{II}(SAr^{iPr6})_2$, **1-Ln**,[26] Ln = La or Nd, with 0.5 equiv. of C_8H_8 resulted in immediate color changes to yellow and green, respectively. After the reaction mixtures were stirred for 1 h and the solvent was removed under reduced pressure, the resulting yellow (La) or dark green (Nd) residues were recrystallized from hexane at −35 °C to afford yellow (La) or green (Nd) crystals of the Ln(III) complexes $Ln^{III}(SAr^{iPr6})(C_8H_8)$, **2-Ln**, eqn (3).

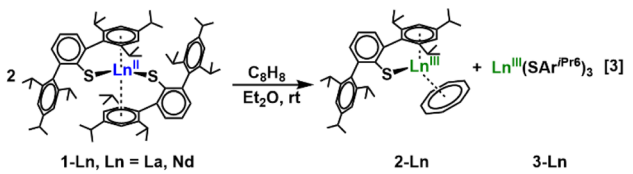

Structure of $Ln^{III}(SAr^{iPr6})(C_8H_8)$, 2-Ln

The molecular structure of **2-Nd** is shown in Fig. 1 (**2-La** is isomorphous, see SI). The metrical parameters of the C_8 ring are consistent with reduction by two electrons. This $(C_8H_8)^{2-}$ ring is planar [sum of internal C–C–C angles of 1080.4(3)° (**2-La**) and 1079.5(9)° (**2-Nd**)] and has Ln—C(C_8H_8) distances in the range of 2.6723(9)-2.7729(9) Å (**2-La**) and 2.614(3)-2.669(3) Å (**2-Nd**). The Ln—C_8H_8 ring centroid distances are 1.989(1) Å (**2-La**) and 1.91(1) Å (**2-Nd**). This distance in **2-La** is somewhat shorter than other neutral La(III) complexes binding a single $(C_8H_8)^{2-}$ ligand, for example 2.094(3) Å in $La(C_5Me_4H)(C_8H_8)(THF)_2$ (ref. 33), while that of **2-Nd** is similar to what is found in other such complexes, *e.g.* 1.90 Å in $Nd(C_5H^iPr_4)(C_8H_8)$.[34]

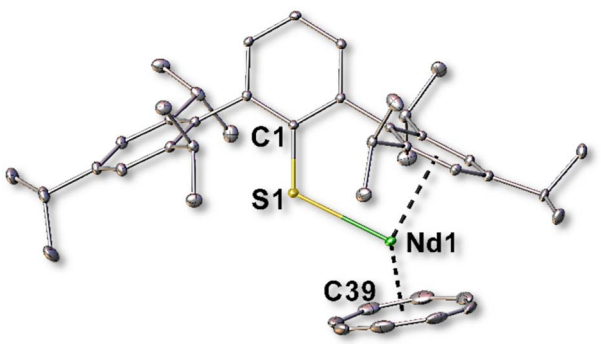

Fig. 1 The molecular structure of $Nd(SAr^{iPr6})(C_8H_8)$, **2-Nd**, with thermal ellipsoids drawn at 30% probability. For clarity, hydrogen atoms and a solvent of crystallization (hexane) are not shown.

In contrast to the precursors **1-Ln**, which have two flanking arene rings oriented in a metallocene-like structure, the **2-Ln** complexes have only one flanking arene ring near the Ln ion. The Ln—Cnt distances of 2.694(1) Å (**2-La**) and 2.633(1)Å (**2-Nd**) are in between the inequivalent values found in **1-La** (2.478(2) and 2.828(2) Å) and **1-Nd** (2.395(1) and 2.804(1) Å). These flanking rings in **2-Ln** are planar with a sum of internal C–C–C angles of 719.9(2)° (**2-La**) and 719.7(5)° (**2-Nd**). In contrast, the flanking rings closest to the metal ion of **1-Ln** (ref. 26) have a boat-like distortion from planarity that is attributed to a δ symmetry interaction between the Ln ion and one flanking ring of a terphenyl. This is also found in the amide analogues of **1-Ln**, $Ln[N(H)Ar^{iPr6}]_2$.[35] The 2.8379(3) Å and 2.7983(6) Å Ln-S distances in **2-La** and **2-Nd**, respectively, are similar to those in $Ln^{III}(SAr^{iPr6})_2I$.[26] Hence, the $(SAr^{iPr6})^{1-}$ ligand functions as an $(XL_3)^{1-}$ ligand in **2-Ln** and these complexes are formulated as Ln(III) species.

Identification of the byproduct of the two electron reduction

Once **2-Ln** was identified, it was important to characterize the byproduct to evaluate the course of the two-electron reduction. Repeated crystallization of the crude material from the reaction in eqn (3) from hexane resulted only in the isolation of crystals of **2-Ln**. However, recrystallization of the same crude material from diethyl ether afforded crystals of both **2-Ln** and $Ln(SAr^{iPr6})_3$, **3-Ln**, the latter of which were suitable for study by X-ray diffraction when mechanically separated from this mixture. To the best of our knowledge, the **3-Ln** species are the first examples of complexes of any element binding three such $(EAr^{iPr6})^{1-}$ ligands (E = O, NH, S, PH). In retrospect, the use this sulfur variant with larger lanthanide ions may be the optimal combination of metal and ligand for forming these tris(ligand) complexes.

The isolation of **3-Ln** is unusual in view of the other products that could possibly form in this reaction, including those involving a bridging $(C_8H_8)^{2-}$ ligand,[36] or a salt of the form $[Ln(SAr^{iPr6})_2][(Ar^{iPr6}S)_2Ln(C_8H_8)]$. A complex of this latter type, $\{Dy[N(H)Ar^{iPr6}]_2\}\{[Ar^{iPr6}N(H)]_2Dy(P_4)\}$ was recently reported from the reaction between the related $Dy[(N(H)Ar^{iPr6})_2]$ and white phosphorus.[37] It is also noteworthy that the **3-Ln** species are rare examples of mononuclear homoleptic tris(thiolate) complexes of the rare-earth elements with any thiolate. The only other structurally characterized examples of this class appear to be $Ln(SC_6H_2$-2,4-6-^{t}Bu$_3)_3$ (Ln = La, Ce, Pr, Nd, and Sm) which were prepared by protonolysis between $Ln[N(SiMe_3)_2]_3$ and the thiol.[38,39]

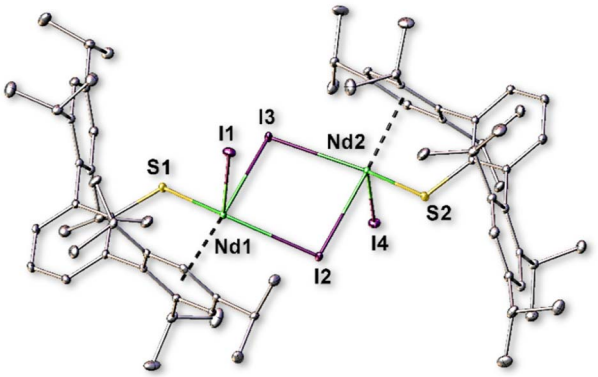

Fig. 2 The molecular structure of $[Nd(SAr^{iPr6})(\mu\text{-}I)(I)]_2$, **4-Nd**, with thermal ellipsoids drawn at 30% probability. For clarity, hydrogen atoms and two molecules of toluene are not shown.

Independent synthesis of $Ln^{III}(SAr^{iPr6})(C_8H_8)$, 2-Ln

Since the similar solubilities of **2-Ln** and **3-Ln** made it difficult to separate them for spectroscopic characterization, independent syntheses of the compounds were pursued. A reasonable synthetic route to **2-Ln** could involve salt metathesis between a dihalide complex like "$Ln(SAr^{iPr6})(I)_2$" with $K_2(C_8H_8)$. Accordingly, we attempted to synthesize di-iodides by the treatment of

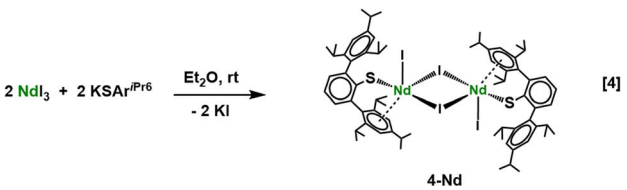

excess LnI_3 with one equiv. of $KSAr^{iPr6}$ in diethyl ether at ambient temperature, eqn (4). The LnI_3 precursors were prepared from the reaction between the rare-earth metal and ammonium iodide as previously described.[40] The LnI_3 synthesis was modified to use a bespoke quartz furnace that allowed the material to be synthesized at large scale in a fume hood. Details of the furnace construction are included in the SI.

Crystallization of the solid residue from the Nd reaction in eqn (4) from toluene afforded the dimeric di-iodide complex $[Nd(SAr^{iPr6})(\mu\text{-}I)(I)]_2$, **4-Nd**, in 68% yield. To date, we have been unable to isolate crystals of the analogous **4-La** that are suitable for study by X-ray diffraction experiments. The molecular structure of **4-Nd** is shown in Fig. 2. The $Nd_2(\mu\text{-}I)_2$ "core" of **4-Nd**

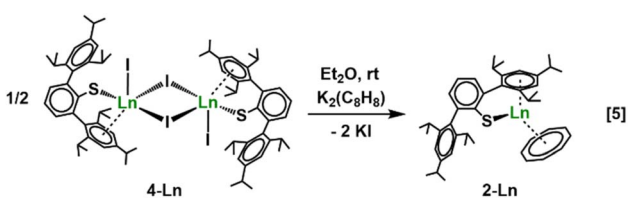

is nearly planar with a sum of interior angles 358.60(3)°. The bridging Nd–I distances range from 3.1154(8)–3.1589 Å, while the terminal Nd–I distances are shorter by *ca.* 0.1 Å, as expected, with values of 2.9999(7) and 3.0031(7) Å. The Ln—S distances of 2.7040(7) and 2.7327(8) Å, are slightly shorter those found in **2-Nd** and $Nd(SAr^{iPr6})_2I$,[26] as expected on the basis of the lower coordination number of the Nd ion in **4-Nd**.

Treatment of a room temperature solution of **4-Nd** with $K_2C_8H_8$ in diethyl ether, eqn (5), afforded **2-Nd** after recrystallization of the residues from hexane. This allowed spectroscopic identification of **2-Nd** and differentiation of the data in mixtures of **2-Nd** and **3-Nd**.

Independent synthesis of $Ln(SAr^{iPr6})_3$, 3-Ln

In our hands, the **3-Ln** complexes could not be prepared by the metathesis between LnI_3 and 3 equiv. of $KSAr^{iPr6}$. Even when the reagents were stirred at 120 °C in toluene for extended periods, the only lanthanide-containing product isolated from this reaction was the previously reported $Ln(SAr^{iPr6})_2I$.[26] Similar difficulties were found in the synthesis of the sterically crowded $(C_5Me)_3Sm$ complex although this highlighted the value of the two-electron reduction in eqn (3) as a synthetic route to new and unusual products.[11,41–43] Thus, we pursued another synthetic route to **3-Ln**.

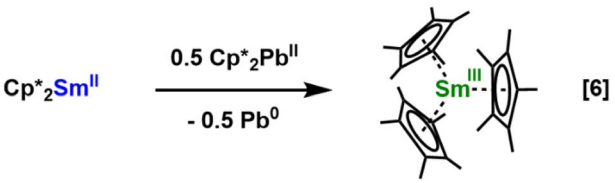

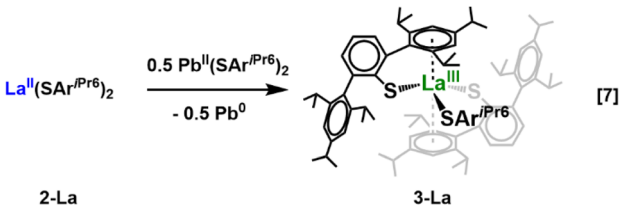

In analogy to the preparation of $Sm(C_5Me_5)_3$ by treatment of $Sm(C_5Me_5)_2$ with $Pb(C_5Me_5)_2$,[41] eqn (6), **1-La** was treated with the bright orange plumbylene $Pb(SAr^{iPr6})_2$, **1-Pb**,[32] in diethyl ether, eqn (7). This reaction proceeded slowly at room temperature, requiring several days for the highly colored solution to diminish in color. Gratifyingly, storage of a filtered diethyl ether solution of this material at −35 °C afforded colorless crystals of **3-La**, although residual plumbylene remained in the product mixture and this route is therefore not a good synthetic route to **3-Ln**.

Structure of $Ln(SAr^{iPr6})_3$

Since the **3-Ln** complexes are the first $Ln(EAr^{iPr6})_3$ complexes of any kind, it was of interest to examine in detail the coordination modes of the three bulky $(SAr^{iPr6})^{1-}$ ligands to the metal.

Table 1 Selected interatomic distances (Å) and angles (°) in Ln(SAr^{iPr6})$_2$I,[26] Ln(SAr^{iPr6})$_2$, **1-Ln**,[26,44] and Ln(SAr^{iPr6})$_2$, **3-Ln**

	Ln(SAr^{iPr6})$_2$I	Ln(SAr^{iPr6})$_2$, **1-Ln**[a]	Ln(SAr^{iPr6})$_2$, **3-Ln**
Ln—S (terminal)	—	—	**3-La:** 2.8709(5) **3-Nd:** 2.780(1)
Ln—S (flanking)	**La:** 2.817(1), 2.824(1) **Nd:** 2.7514(6), 2.7720	**1-La:** 2.797(2), 2.837(2) **1-Nd:** 2.741(1), 2.776(1)	**3-La:** 2.8310(4), 2.8327(4) **3-Nd:** 2.7404(9), 2.791(1)
Ln—Cnt	**La:** 2.808(2), 2.817(2) **Nd:** 2.793(1), 2.799(1)	**1-La:** 2.478(2), 2.828(2) **1-Nd:** 2.395(1), 2.805(1)	**3-La:** 2.766(1), 2.951(1) **3-Nd:** 2.61(2), 3.36(2)
S—Ln—S	**La:** 125.32(3) **Nd:** 127.39(2)	**1-La:** 137.06(2) **1-Nd:** 140.36(3)	**3-La:** 111.10(1), 118.38(1), 130.49(1) **3-Nd:** 109.97(3), 117.74(3), 130.57(3)
Cnt—Ln—Cnt	**La:** 173.20(5) **Nd:** 175.39(3)	**1-La:** 168.74(7) **1-Nd:** 164.67(5)	**3-La:** 161.89(2) **3-Nd:** 156.06(4)

[a] The structures of **1-Ln** are crystallographically disordered at the Ln site. The above values describe only the major (80%) component. The shorter of the two Ln—Cnt distances in **1-Ln** are associated with a δ-bonding interaction between the Ln ion and a flanking arene ring.

Selected bond metrics of Ln(SAr^{iPr6})$_2$I, **1-Ln**, and **3-Ln** are provided in Table 1.

The molecular structure of **3-La** is shown in Fig. 3. The coordination environment of La in **3-La** is similar to the previously reported iodide complex La(SAr^{iPr6})$_2$I[26] in which the La atom lies in the plane formed by the three atoms that are σ-bonded to the metal. A flanking arene ring from each of two terphenylthiolate ligands is oriented toward the La ion to form a sandwich-like complex, but in **3-La** the 161.89(2)° Cnt—La—Cnt angle is significantly smaller than the corresponding 173.22(5)° angle in La(SAr^{iPr6})$_2$I. This is consistent with increased steric crowding. A further distortion involves the La—centroid distances which are similar in La(SAr^{iPr6})$_2$I (2.809(2) and 2.817(2) Å), but differ by *ca.* 0.20 Å in **3-La** with values of 2.766(1) and 2.951(1) Å. In contrast, the 2.8310(4) Å La1–S2 and 2.8327(4) Å La1–S3 distances of **3-La** are similar and only slightly shorter than the 2.8709(5) Å La1–S1 distance of the terphenylthiolate ligand that binds to La only through a sulfur atom in **3-La**.

The overall structure of **3-Nd**, Fig. 4, is similar to that of **3-La**, but it features several differences likely arising from the smaller ionic radius of Nd.[45] The 156.06(4)° Cnt—Nd—Cnt angle is even more bent than in **3-La**, and there is an even larger difference in the Nd—Cnt distances: 2.61(2) and 3.36(2) Å. While the flanking ring associated with the longer of these two distances is oriented toward the Nd ion, this distance is exceptionally long and thus any interaction between the Nd ion and this arene ring is likely very weak (*cf.* Nd—Cnt distances of 2.799(1) and 2.793(1) Å in Nd(SAr^{iPr6})$_2$I[26]). An additional difference is that the Nd ion of **3-Nd** is situated out of the plane formed by the three sulfur atoms by 0.209(1) Å compared to the planar arrangement found in **3-La**. Interestingly, the 2.780(1) Å Nd1—S1, the 2.791(1) Å Nd1—S2, and the 2.7405(9) Å Nd1—S3 bonds are of similar

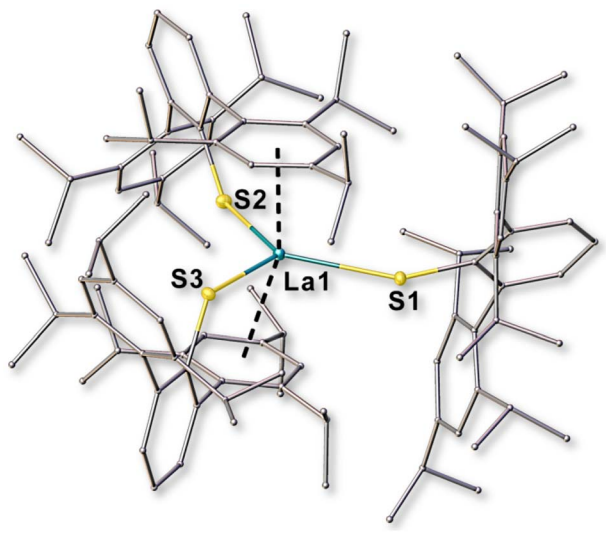

Fig. 3 The molecular structure of La(SAr^{iPr6})$_3$, **3-La**, with selected thermal ellipsoids drawn at 30% probability. For clarity, hydrogen atoms and a solvent of crystallization (diethyl ether) are not shown and the terphenyl framework has been drawn in wireframe. Full structural details are given in the SI.

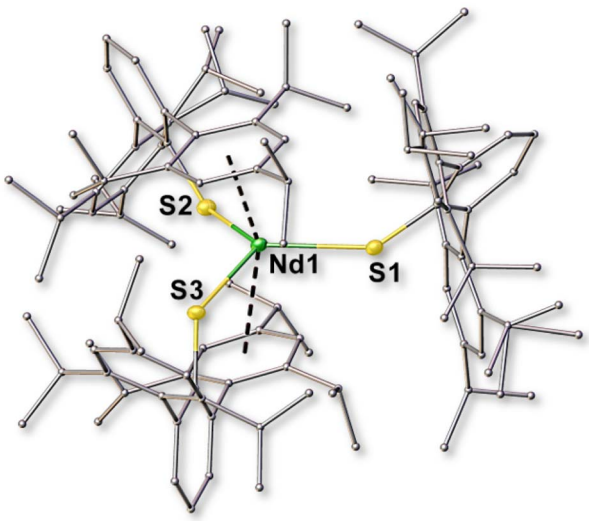

Fig. 4 The molecular structure of Nd(SAr^{iPr6})$_3$, **3-Nd**, with selected thermal ellipsoids drawn at 20% probability. For clarity, hydrogen atoms and a solvent of crystallization (diethyl ether) are not shown and the terphenyl framework has been drawn in wireframe. Full structural details are given in the SI.

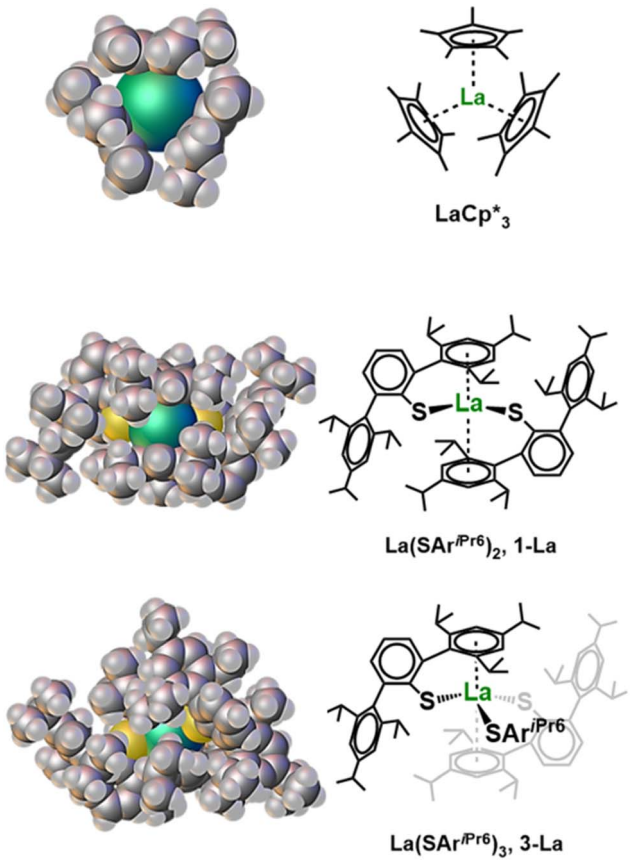

Fig. 5 Space-filling models of $LaCp^*_3$ (top), $La(SAr^{iPr6})_2$ (**1-La**, middle), and $La(SAr^{iPr6})_3$ (**3-La**, bottom) with spheres drawn at 100% of their van der Waals radii. Each molecule has been oriented to show the most exposed region of the La coordination sphere.

length although the coordination of their flanking rings is very different. This is also found in **3-La** and suggests that the Ln—S bonds maintain a narrow distance range while the arene ring coordination can be highly variable.

To evaluate steric crowding in the structure of **3-La**, space-filling models were compared to the bis(thiolate) $La^{II}(SAr^{iPr6})_2$, **1-La**, and the quintessential sterically crowded $(C_5Me_5)_3La$, Fig. 5. One means of quantifying the steric crowding around a metal ion is to calculate the Guzei *G* parameter, which is an estimation of the percentage of the coordination sphere of a metal ion that is covered by the ligands.[46] The calculated *G* value for both **3-Ln** complexes is 97%, while the corresponding value for the Ln(II) complexes $Ln(SAr^{iPr6})_2$, **1-Ln**, is substantially lower at 89%. In comparison, the first tris(pentamethylcyclopentadienyl) complex of any element, $(C_5Me_5)_3Sm$,[11] has a *G* value of only 81% and the analogous $(C_5Me_5)_3La$ has a *G* value of 80%. Presumably the greater coordinative flexibility of the $(SAr^{iPr6})^{1-}$ ligands compared to the planar $(C_5Me_5)^{1-}$ allows the terphenylthiolates to more completely saturate the coordination sphere of the metal.

Closer inspection of the structures of **3-Ln** reveals that the terphenyl ligand which binds the Ln ion solely through the sulfur atom is slightly distorted as a result of the crowding in the molecule. Thus, the flanking arene rings of this ligand are bent away from the rest of the molecule with C(central ring *ortho*)—C(flanking ring *ipso*)—C(flanking ring *para*) angles that deviate from linearity by 7.4(2)° and 16.3(2)° in **3-La** and 7.3(3)° and 10.3(3)° in **3-Nd**; the analogous angles in the remaining ligands of the **3-Ln** complexes deviate from linearity by less than 6°. Such bending within these ligands is reminiscent of the out-of-plane methyl carbon atoms that are present in the structures of the $(C_5Me_5)_3Ln$ complexes.[11]

Structural indications of London dispersion effects (LDEs) in 3-Ln

Although the distortions in the terphenyl framework of the terminal thiolate ligand are clear evidence of interligand repulsion, the **3-Ln** structures contain multiple interligand C···C contacts among the methyl carbons of the ligands that are shorter than the sum of the van der Waals radii of two methyl groups (vdW radius of $-CH_3 = 2.0$ Å).[47] While steric crowding in organometallic molecules has long been known to result in interligand repulsion, a growing body of research has shown that such close interactions between ligand hydrocarbon moieties are in many cases indicative of attractive London dispersion effects (LDEs) that can contribute to the stability of a molecule.[48–52] In some striking cases, these effects are critical to the formation and stability of a molecule.[53,54] For example, attractive interligand LDEs were calculated to contribute stabilizations of *ca.* 20–30 kcal mol^{-1} in the linearly coordinated transition metal amide complexes M[N(SiMe$_3$)Dipp] (M = Fe, Co, or N; Dipp = C_6H_3-2,6-^{i}Pr$_2$).[55] Other cases showed substantial contributions from LDEs to the bonding interaction between two metals: LDEs were calculated to contribute *ca.* 50% of the interaction energy between the metal atoms in β-

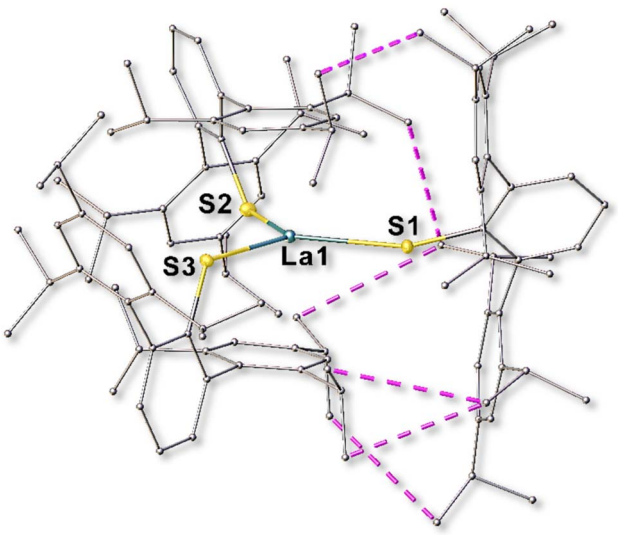

Fig. 6 The molecular structure of $La(SAr^{iPr6})_3$, **3-La**, with dashed lines in pink which indicate short (<4.0 Å) C···C approaches between methyl carbons of the terminally bound terphenylthiolate ligand and those of the remaining two ligands. For clarity, hydrogen atoms and a solvent of crystallization (diethyl ether) are not shown.

diketiminate complexes featuring Cu–Al or Cu–Ga bonds,[56] and dispersion-corrected calculations afforded a ΔG of dimerization of −6.1 kcal mol^{-1} in the distannene [Sn(C$_6$H$_2$-2,4,6-Cy$_3$)$_2$]$_2$ (Cy = cyclohexyl); excluding LDEs from these calculations afforded a ΔG of dimerization of +31.9 kcal mol^{-1}.[57] Similar effects relevant to this work were observed in a series of terphenyl-substituted diplumbynes, where exclusion of LDEs from the calculated Pb–Pb interaction energies showed that these dimeric lead complexes were unstable toward dissociation in the absence of these attractive interactions.[58]

In the structure of **3-La**, six C⋯C contacts between the methyl carbons of the terminal terphenylthiolate ligand and those of the other two ligands were identified which are shorter than 4.0 Å, Fig. 6. Eight such contacts were found in the structure of **3-Nd**. While single approaches of this kind contribute very little to interligand attraction, the cumulative effect of many such contacts can amount to an attraction of several tens of kcal mol^{-1}.[49,52,59,60] Additionally, the high polarizability of the alkyl-substituted terphenyl framework increases the probability that such close contacts can result in attractive interactions.[61,62] Thus, although more data are required to explore this effect in complexes like **3-Ln**, the many close interligand C⋯C contacts found in **3-Ln** are an experimental indicator of the likely contribution of LDEs to the stability of these unusually crowded molecules.

Evaluation of London dispersion effects (LDEs) by density functional theory (DFT)

To examine the contribution of LDEs further, the **3-Ln** complexes were studied computationally by DFT. Geometry optimizations were performed on the structures obtained from single crystal X-ray diffraction experiments with hexane solvation effects using the COSMO model[63] with a dielectric constant of 1.887 and a refractive index of 1.3727. Split-valence basis sets with polarization functions on all non-hydrogen atoms, def2-SV(P),[64] were used for C, H, S atoms, and triple-zeta quality basis sets, def2-TZVP,[65] were used for La and Nd with scalar-relativistic effective core potentials (46 core electrons for La and 28 core electrons for Nd, def2-ecp[66]). The TPSSh[67] functional with D4 dispersion corrections[68] was used to optimize the structures in the solution phase. Singlet and triplet instability analyses[69] were also performed for closed shell singlet states. A numerical quadrature grid[70] of size 4 and weight derivatives were used for exchange-correlation integrals. Ground state energies were converged with a threshold of 10^{-7} a.u. and the Cartesian energy gradient had a maximum norm of 10^{-4} a.u. Kohn–Sham orbitals corresponding to different spin states of each structure. Local minima on the potential energy surface were confirmed by numerical force constant calculations.[71] The VMD program[72] was used to visualize molecular orbitals with a contour value of 0.03.

The geometry optimized structures were in good agreement with their experimental counterparts (see SI for details). When corrected for dispersion (D4),[68] the calculations for **3-La** indicated that the dissociation energy of the terminally bound (SAr^{iPr6})$^{1-}$ ligand amounts to 89 kcal mol^{-1}. These calculations further indicated that the contribution of LDEs to this dissociation energy amounts to 48 kcal mol^{-1}. In other words, approximately half of the dissociation energy of the terminal (SAr^{iPr6})$^{1-}$ ligand in **3-La** is due to dispersion effects. Similar results were found for **3-Nd**, for which the total dissociation energy of the terminal (SAr^{iPr6})$^{1-}$ ligand was calculated to be 96 kcal mol^{-1} with a dispersion contribution of 48 kcal mol^{-1}.

The dissociation energies for the two ligands of **3-La** which are bound to the La atom through both a sulfur atom and a flanking arene ring were calculated to be 96 and 91 kcal mol^{-1}. The higher dissociation energy is associated with the terphenylthiolate ligand with the shorter La—Cnt distance, 2.776(1) Å, and the lower energy is associated with the longer La—Cnt distance of 2.951(1) Å. The contribution of dispersion effects to these energies was calculated to be 48 kcal mol^{-1} in both cases. For **3-Nd**, the dissociation energies for the analogous ligands were calculated to be 85 and 83 kcal mol^{-1}. As with **3-La**, the higher dissociation energy is associated with the ligand which has the shorter Nd—Cnt distance and the contribution of dispersion effects to each of these energies again amounts to 48 kcal mol^{-1}. The uniformity of the dispersion contribution is reasonable because the LDEs are the result of mutual interactions between all of the ligands. It is remarkable that, due to LDEs, the calculated interaction energy between the Ln ion and the terminal terphenylthiolate ligand is similar to that of the other two ligands in **3-Ln** despite the absence of any apparent Ln—arene interaction between the terminal terphenylthiolate ligand and the Ln ion. Previous NMR studies by Niemeyer estimated an Yb–arene interaction energy of *ca.* 13 kcal mol^{-1} in **1-Yb**.[73]

The contribution of LDEs to these interactions is on the high end of such values that have been calculated to date.[48,49,52] This is likely a consequence of the large number of close C⋯C contacts that are available in the **3-Ln** molecules as a result of the Ln ion binding three highly substituted terphenylthiolate ligands. This result is particularly surprising in view of the very large ionic radii of the lanthanide elements and the fact that the attraction due to LDEs is proportional to r^{-6}, where r is the distance between two interacting closed-shell components.[74,75] Thus, while the **3-Ln** molecules are highly crowded and experience a high degree of steric repulsion as indicated by the aforementioned structural distortions, these calculations indicated that LDEs arising from the bulky terphenylthiolate ligands have a substantial effect on these complexes.

Conclusions

The formation of Ln(SAr^{iPr6})$_2$(C$_8$H$_8$), **2-Ln**, from the reduction of cyclooctatetraene to (C$_8$H$_8$)$^{2-}$ by Ln(SAr^{iPr6})$_2$ shows the potential of complexes of the (SAr^{iPr6})$^{1-}$ ligand platform to accomplish two-electron reduction reactivity with Ln(II) compounds similar to that previously known for metallocene complexes of Sm(II). The Ln(SAr^{iPr6})$_2$ species can function as 1- or 2-electron reductants depending on the substrate and the stoichiometry used.[26] In addition, the two-electron reduction chemistry of Ln(SAr^{iPr6})$_2$ has provided access to the first examples of M(EAr^{iPr6})$_3$ complexes of any kind (M = any element; E = O, NH, S, PH). The

differing structures of **3-La** and **3-Nd** demonstrate the adaptability of the $(SAr^{iPr6})^{1-}$ ligands to accommodate steric crowding that can vary with the size of the metal in the complex. The results on **3-Ln** also show the importance of the multiple short interligand C⋯C contacts in **3-Ln** that are indicators of the role that LDEs can play in the formation of unusual $(SAr^{iPr6})^{1-}$ complexes and rare-earth complexes more generally. For **3-Ln**, DFT calculations are consistent with this: this study showed that LDEs are responsible for about half of the strength of the interaction between the Ln ion and each of the ligands. Overall, these results suggest that the flexibility of the $(SAr^{iPr6})^{1-}$ ligand, both electronically and sterically, as well as its dispersion effect donation ability, can provide a wide range of reactivity to the rare-earth metals that can lead to new classes of complexes and new types of reactions.

Author contributions

MRL and CRS contributed equally to this work.

Conflicts of interest

There are no conflicts to declare.

Data availability

The data supporting this article have been included as part of the supplementary information (SI). Supplementary information is available. See DOI: https://doi.org/10.1039/d6sc00248j.

CCDC 2448128 (**2-La·hexane**), 2463799 (**2-La**), 2340165 (**2-Nd**), 2432906 (**3-La**), 2439964 (**3-Nd**), and 2391514 (**4-Nd**) contain the supplementary crystallographic data for this paper.[76a–f]

Acknowledgements

The authors thank the U. S. National Science Foundation for support of this research under CHE-2452677 (to WJE for the experimental research), and CHE-2503294 (to FF for the theoretical studies).

Notes and references

1 R. E. Connick, *J. Chem. Soc.*, 1949, S235–S241.
2 W. J. Evans, *Coord. Chem. Rev.*, 2000, **206–207**, 263–283.
3 S. Cotton, *The Lanthanides - Principles and Energetics*, 2006.
4 J. C. Wedal and W. J. Evans, *J. Am. Chem. Soc.*, 2021, **143**, 18354–18367.
5 C. Elschenbroich, *Organometallics*, Wiley-VCH, Weinheim, 3rd edn, 2006.
6 R. H. Crabtree, *The Organometallic Chemistry of the Transition Metals*, John Wiley & Sons, Inc., 2014.
7 J. F. Hartwig, *Organotransition Metal Chemistry : From Bonding to Catalysis*, University Science Books, Mill Valley, Calif., 2010.
8 T. Behrsing, G. B. Deacon and P. Junk, in *The Lanthanides and Actinides*, World Scientific, Europe, 2021, pp. 1–36.
9 W. J. Evans, J. W. Grate, L. A. Hughes, H. Zhang and J. L. Atwood, *J. Am. Chem. Soc.*, 1985, **107**, 3728–3730.
10 T. Simler, K. N. McCabe, L. Maron and G. Nocton, *Chem. Sci.*, 2022, **13**, 7449–7461.
11 W. J. Evans, S. L. Gonzales and J. W. Ziller, *J. Am. Chem. Soc.*, 1991, **113**, 7423–7424.
12 C. E. Davies, I. M. Gardiner, J. C. Green, M. L. H. Green, N. J. Hazel, P. D. Grebenik, V. S. B. Mtetwa and K. Prout, *J. Chem. Soc., Dalton Trans.*, 1985, 669–683.
13 T. D. Tilley and R. A. Andersen, *Inorg. Chem.*, 1982, **20**, 3267–3270.
14 J. Marçalo and A. P. De Matos, *Polyhedron*, 1989, **8**, 2431–2437.
15 M. R. MacDonald, J. E. Bates, M. E. Fieser, J. W. Ziller, F. Furche and W. J. Evans, *J. Am. Chem. Soc.*, 2012, **134**, 8420–8423.
16 M. R. MacDonald, J. E. Bates, J. W. Ziller, F. Furche and W. J. Evans, *J. Am. Chem. Soc.*, 2013, **135**, 9857–9868.
17 A. C. Boggiano, C. M. Studvick, S. Roy Chowdhury, J. E. Niklas, H. Tateyama, H. Wu, J. E. Leisen, F. Kleemiss, B. Vlaisavljevich, I. A. Popov and H. S. La Pierre, *Nat. Chem.*, 2025, **17**, 1005–1010.
18 A. C. Boggiano, S. R. Chowdhury, M. D. Roy, M. G. Bernbeck, S. M. Greer, B. Vlaisavljevich and H. S. La Pierre, *Angew. Chem., Int. Ed.*, 2024, **63**, e202409789.
19 A. R. Willauer, C. T. Palumbo, R. Scopelliti, I. Zivkovic, I. Douair, L. Maron and M. Mazzanti, *Angew. Chem., Int. Ed.*, 2020, **59**, 3549–3553.
20 M. Tricoire, W. Sroka, T. Rajeshkumar, R. Scopelliti, A. Sienkiewicz, L. Maron and M. Mazzanti, *J. Am. Chem. Soc.*, 2025, **147**, 1162–1171.
21 M. N. Bochkarev, I. L. Fedushkin, S. Dechert, A. A. Fagin and H. Schumann, *Angew. Chem., Int. Ed.*, 2001, **40**, 3176–3178.
22 M. N. Bochkarev, I. L. Fedushkin, A. A. Fagin, T. V. Petrovskaya, J. W. Ziller, R. N. R. Broomhall-Dillard and W. J. Evans, *Angew. Chem., Int. Ed.*, 1997, **36**, 133–135.
23 C. R. Stennett, J. Q. Nguyen, J. W. Ziller and W. J. Evans, *Organometallics*, 2023, **42**, 696–707.
24 C. Camp, V. Guidal, B. Biswas, J. Pcaut, L. Dubois and M. Mazzanti, *Chem. Sci.*, 2012, **3**, 2433–2448.
25 E. J. Coughlin, M. Zeller and S. C. Bart, *Angew. Chem., Int. Ed.*, 2017, **56**, 12142–12145.
26 K. Gilbert-Bass, C. R. Stennett, R. Grotjahn, J. W. Ziller, F. Furche and W. J. Evans, *Chem. Commun.*, 2024, **60**, 4601–4604.
27 G. B. Deacon, S. Nickel, P. Mackinnon and E. R. T. Tiekink, *Aust. J. Chem.*, 1990, **43**, 1245–1257.
28 G. B. Deacon, C. M. Forsyth, P. C. Junk, B. W. Skelton and A. H. White, *Chem.–Eur. J.*, 1999, **5**, 1452–1459.
29 G. B. Deacon, P. C. Junk, G. J. Moxey, K. Ruhlandt-Senge, C. St. Prix and M. F. Zuniga, *Chem.–Eur. J.*, 2009, **15**, 5503–5519.
30 G. B. Deacon, P. C. Junk and G. J. Moxey, *Chem.–Asian J.*, 2009, **4**, 1309–1317.
31 B. L. L. Réant, J. A. Seed, G. F. S. Whitehead and C. A. P. Goodwin, *Inorg. Chem.*, 2025, **64**, 3161–3177.

32 B. D. Rekken, T. M. Brown, J. C. Fettinger, F. Lips, H. M. Tuononen, R. H. Herber and P. P. Power, *J. Am. Chem. Soc.*, 2013, **135**, 10134–10148.
33 H. Schumann, M. Glanz, J. Winterfeld and H. Hemling, *J. Organomet. Chem.*, 1993, **456**, 77–83.
34 M. Visseaux, D. Barbier-Baudry, O. Blacque, A. Hafid, P. Richard and F. Weber, *New J. Chem.*, 2000, **24**, 939–942.
35 R. E. MacKenzie, T. Hajdu, J. A. Seed, G. F. S. Whitehead, R. W. Adams, N. F. Chilton, D. Collison, E. J. L. McInnes and C. A. P. Goodwin, *Chem. Sci.*, 2024, **15**, 15160–15169.
36 W. J. Evans, M. A. Johnston, R. D. Clark and J. W. Ziller, *J. Chem. Soc., Dalton Trans.*, 2000, 1609–1612.
37 R. Jena, F. Benner, R. J. Staples, S. Demir and A. L. Odom, *Inorg. Chem.*, 2025, **64**, 20643–20651.
38 B. Çetinkaya, P. B. Hitchcock, M. F. Lappert and R. G. Smith, *J. Chem. Soc., Chem. Commun.*, 1992, 932–934.
39 M. Roger, N. Barros, T. Arliguie, P. Thuéry, L. Maron and M. Ephritikhine, *J. Am. Chem. Soc.*, 2006, **128**, 8790–8802.
40 C. R. Stennett, M. R. Luevano, J. D. Queen, J. Q. Nguyen, W. N. G. Moore and W. J. Evans, *Inorg. Chem.*, 2024, **63**, 16855–16860.
41 W. J. Evans, K. J. Forrestal, J. T. Leman and J. W. Ziller, *Organometallics*, 1996, **15**, 527–531.
42 W. J. Evans, K. J. Forrestal and J. W. Ziller, *Angew. Chem., Int. Ed.*, 1997, **36**, 774–776.
43 W. J. Evans, C. A. Seibel and J. W. Ziller, *J. Am. Chem. Soc.*, 1998, **120**, 6745–6752.
44 M. R. Luevano, C. R. Stennett, E. Ma, J. W. Ziller, F. Furche and W. J. Evans, *J. Am. Chem. Soc.*, 2025, **147**, 34249–34255.
45 R. D. Shannon, *Acta. Crystallogr. Sect. A*, 1976, **32**, 751–767.
46 I. A. Guzei and M. Wendt, *Dalton Trans.*, 2006, 3991–3999.
47 L. Pauling, *The Nature of the Chemical Bond*, Cornell University Press, Ithaca, New York, 3rd edn, 1960.
48 D. J. Liptrot, J.-D. Guo, S. Nagase and P. P. Power, *Angew. Chem., Int. Ed.*, 2016, **55**, 14766–14769.
49 D. J. Liptrot and P. P. Power, *Nat. Rev. Chem.*, 2017, **1**, 4.
50 M. Bursch, E. Caldeweyher, A. Hansen, H. Neugebauer, S. Ehlert and S. Grimme, *Acc. Chem. Res.*, 2019, **52**, 258–266.
51 P. P. Power, *Organometallics*, 2020, **39**, 4127–4138.
52 K. L. Mears and P. P. Power, *Acc. Chem. Res.*, 2022, **55**, 1337–1348.
53 C. L. Wagner, L. Tao, E. J. Thompson, T. A. Stich, J. Guo, J. C. Fettinger, L. A. Berben, R. D. Britt, S. Nagase and P. P. Power, *Angew. Chem., Int. Ed.*, 2016, **55**, 10444–10447.
54 A. Casitas, J. A. Rees, R. Goddard, E. Bill, S. DeBeer and A. Fürstner, *Angew. Chem., Int. Ed.*, 2017, **56**, 10108–10113.
55 C.-Y. Lin, J.-D. Guo, J. C. Fettinger, S. Nagase, F. Grandjean, G. J. Long, N. F. Chilton and P. P. Power, *Inorg. Chem.*, 2013, **52**, 13584–13593.
56 K. L. Mears, C. R. Stennett, E. K. Taskinen, C. E. Knapp, C. J. Carmalt, H. M. Tuononen and P. P. Power, *J. Am. Chem. Soc.*, 2020, **142**, 19874–19878.
57 C. R. Stennett, M. Bursch, J. C. Fettinger, S. Grimme and P. P. Power, *J. Am. Chem. Soc.*, 2021, **143**, 21478–21483.
58 J. D. Queen, M. Bursch, J. Seibert, L. R. Maurer, B. D. Ellis, J. C. Fettinger, S. Grimme and P. P. Power, *J. Am. Chem. Soc.*, 2019, **141**, 14370–14383.
59 S. Rsel, C. Balestrieri and P. R. Schreiner, *Chem. Sci.*, 2017, **8**, 405–410.
60 J. P. Wagner and P. R. Schreiner, *Angew. Chem., Int. Ed.*, 2015, **54**, 12274–12296.
61 G. P. Chen, V. K. Voora, M. M. Agee, S. G. Balasubramani and F. Furche, *Annu. Rev. Phys. Chem.*, 2017, **68**, 421–445.
62 J. F. Dobson and T. Gould, *J. Phys.: Condens. Matter*, 2012, **24**, 073201.
63 A. Klamt and G. Schüürmann, *J. Chem. Soc. Perkin Trans. 2*, 1993, 799–805.
64 A. Schäfer, H. Horn and R. Ahlrichs, *J. Chem. Phys.*, 1992, **97**, 2571–2577.
65 F. Weigend and R. Ahlrichs, *Phys. Chem. Chem. Phys.*, 2005, **7**, 3297–3305.
66 M. Dolg, H. Stoll and H. Preuss, *J. Chem. Phys.*, 1989, **90**, 1730–1734.
67 V. N. Staroverov, G. E. Scuseria, J. Tao and J. P. Perdew, *J. Chem. Phys.*, 2003, **119**, 12129–12137.
68 E. Caldeweyher, S. Ehlert, A. Hansen, H. Neugebauer, S. Spicher, C. Bannwarth and S. Grimme, *J. Chem. Phys.*, 2019, **150**, 154122.
69 R. Bauernschmitt and R. Ahlrichs, *J. Chem. Phys.*, 1996, **104**, 9047–9052.
70 O. Treutler and R. Ahlrichs, *J. Chem. Phys.*, 1995, **102**, 346–354.
71 P. Deglmann, K. May, F. Furche and R. Ahlrichs, *Chem. Phys. Lett.*, 2004, **384**, 103–107.
72 W. Humphrey, A. Dalke and K. Schulten, *J. Molec. Graphics*, 1996, **14**, 33–38.
73 M. Niemeyer, *Eur. J. Inorg. Chem.*, 2001, **2001**, 1969–1981.
74 R. Eisenschitz and F. London, *Z. Phys.*, 1930, **60**, 491–527.
75 D. G. Truhlar, *J. Chem. Educ.*, 2019, **96**, 1671–1675.
76 (*a*) CCDC 2448128: Experimental Crystal Structure Determination, 2026, DOI: 10.5517/ccdc.csd.cc2n5gw6; (*b*) CCDC 2463799: Experimental Crystal Structure Determination, 2026, DOI: 10.5517/ccdc.csd.cc2npsdk; (*c*) CCDC 2340165: Experimental Crystal Structure Determination, 2026, DOI: 10.5517/ccdc.csd.cc2jk46g; (*d*) CCDC 2432906: Experimental Crystal Structure Determination, 2026, DOI: 10.5517/ccdc.csd.cc2mnmvs; (*e*) CCDC 2439964: Experimental Crystal Structure Determination, 2026, DOI: 10.5517/ccdc.csd.cc2mwzj1; (*f*) CCDC 2391514: Experimental Crystal Structure Determination, 2026, DOI: 10.5517/ccdc.csd.cc2l8km2.